Role of amino acid 159 in carbapenem and temocillin hydrolysis of OXA-933, a novel OXA-48 variant

Mariam Rima, Saoussen Oueslati, Garance Cotelon, Elodie Creton, Rémy Bonnin, Laurent Dortet, Bogdan I. Iorga, Thierry Naas

▶ **To cite this version:**

Mariam Rima, Saoussen Oueslati, Garance Cotelon, Elodie Creton, Rémy Bonnin, et al.. Role of amino acid 159 in carbapenem and temocillin hydrolysis of OXA-933, a novel OXA-48 variant. Antimicrobial Agents and Chemotherapy, 2024, 68 (5), pp.e0018024. 10.1128/aac.00180-24 . hal-04766139

HAL Id: hal-04766139
https://hal.science/hal-04766139v1

Submitted on 4 Nov 2024

HAL is a multi-disciplinary open access archive for the deposit and dissemination of scientific research documents, whether they are published or not. The documents may come from teaching and research institutions in France or abroad, or from public or private research centers.

L'archive ouverte pluridisciplinaire **HAL**, est destinée au dépôt et à la diffusion de documents scientifiques de niveau recherche, publiés ou non, émanant des établissements d'enseignement et de recherche français ou étrangers, des laboratoires publics ou privés.

Role of Amino-Acid 159 in carbapenem and temocillin hydrolysis of OXA-933, a novel OXA-48 variant

Mariam Rima[1], Saoussen Oueslati[1,2], Garance Cotelon[3], Elodie Creton[3], Rémy A. Bonnin[1,3], Laurent Dortet,[1,2,3] Bogdan I. Iorga,[4] Thierry Naas[1,2,3]

[1] Team ReSIST, INSERM U1184, School of Medicine Université Paris-Saclay, LabEx LERMIT, Le Kremlin-Bicêtre, France

[2] Bacteriology-Hygiene unit, Assistance Publique/Hôpitaux de Paris, Bicêtre Hospital, Le Kremlin-Bicêtre, France

[3] French National Reference Center for Antibiotic Resistance: Carbapenemase-producing Enterobacterales, Le Kremlin-Bicêtre, France

[4] Université Paris-Saclay, CNRS UPR 2301, Institut de Chimie des Substances Naturelles, Gif-sur-Yvette, France.

Running title : OXA-933, a D159N variant of OXA-48

Keywords: Resistance carbapenems, Carbapenemase, OXA-48-like, Enterobacterales carbapenemase-producer

* Corresponding author: Service de Bactériologie-Hygiène, Hôpital Bicêtre, 78 rue du Général Leclerc, 94270 Le Kremlin-Bicêtre, France. Tel: +33 1 45 21 20 19. Fax: +33 1 45 21 63 40. E-mail: thierry.naas@aphp.fr

Abstract

OXA-48 has rapidly disseminated worldwide and became one of the most common carbapenemase in many countries with more than 45 variants reported with in some cases significant differences in their hydrolysis profiles. The R214 residue, located in the ß5-ß6 loop, is crucial for the carbapenemase activity, as it stabilizes carbapenems in the active site and maintains the shape of the active site through interactions with D159. In this study, we have characterized a novel variant of OXA-48, OXA-933 with a single D159N change. To evaluate the importance of this residue, point mutations were generated (D159A, D159G, D159K, D159W), kinetic parameters of OXA-933, OXA-48 D159G, and OXA-48 D159K were determined and compared to those of OXA-48 and OXA-244. The *bla*$_{\text{OXA-933}}$ gene was borne on Tn*2208*, a 2696-bp composite transposon made of two IS*1* elements surrounded by 9-bp target site duplications and inserted into a non self-transmissible plasmid pOXA-933 of 7872-bp in size. MIC values of *E. coli* expressing *bla*$_{\text{OXA-933}}$ gene or of its point mutant derivatives were lower for carbapenems (except for D159G) as compared to those expressing *bla*$_{\text{OXA-48}}$ gene. Steady state kinetic parameters revealed lower catalytic efficiencies for expanded spectrum cephalosporins and carbapenems. A detailed structural analysis confirmed the crucial role of D159 in shaping the active site of OXA-48 enzymes by interacting with R214. Our work further illustrates the remarkable propensity of OXA-48-like carbapenemases to evolve through mutations at positions outside the β5-β6 loop, but interacting with key residues of it.

Introduction

Carbapenemase producing Enterobacterales constitute a serious health issue limiting the therapeutic options for gram-negative bacterial infections and increasing the morbidity and mortality rates among patients (1). Carbapenemases belong to three molecular classes of ß-lactamases (1,2). Class A and D correspond to serine-active ß-lactamases and class B enzymes are metallo-ß-lactamases that require two Zn^{2+} ions to coordinate a water molecule in the active site for hydrolysis (1,3). Among Carbapenem-Hydrolyzing class D β-Lactamase (CHDL), OXA-48, initially described in 2004, in a carbapenem-resistant *Klebsiella pneumoniae* isolate from Turkey in 2001, has now spread globally in Enterobacterales, to become the most common carbapenemase in many countries (4-6). OXA-48 hydrolyzes penicillins at a high level, carbapenems at a low level and lacks significant hydrolytic activity towards expanded-spectrum cephalosporin (ESC) (6-7). More than 45 variants have since been reported, differing by a few amino acid substitutions or deletions (Beta-Lactamase DataBase http://bldb.eu/BLDB.php?class=D#OXA; 8). While some OXA-48-variants with single amino acid substitutions have similar hydrolytic profiles as OXA-48, others, especially those with changes in the ß5-ß6 loop located close to the substrate binding site, which represents 22/45 of described variants, have significant changes in the hydrolytic spectrum of ß-lactams (7,8). This is the case for variants with a change at position R214, such as OXA-244 (R214G) and OXA-232 (R214S) that have decreased carbapenemase activity (7,9), but also for variants with a four-amino-acid deletion inside the loop such as OXA-163 or OXA-405, which results in the loss of carbapenemase activity and a gain of the ability to hydrolyze oxyimino-cephalosporins (10,11). Finally, other variants such as OXA-438, OXA-517 and OXA-793 with two AA deletions in the

β5–β6 loop, have been described with the ability to hydrolyze carbapenems and oxyimino-cephalosporins equally well (12-14).

The overall 3D structure of OXA-48 is very similar to that of other class D beta-lactamases (DBLs) (15,16), with however one main difference, e.g. an overall shorter the β5 and β6 strands (15,16). Consequently, the β5–β6 loop has a different orientation from that found in other DBLs. The observed conformation of the loop in OXA-48 is promoted by a salt bridge of R214 with the Ω-loop D159 residue, which itself is stabilized by S155 (15-18). In 16 out the 22 OXA-48 variants with changes in the ß5-ß6 loop, the R214 is changed to S (n=3), G (n=3), N (n=1), D (n=3), K (n=1), E (n=2), and G (n=3) (8). In 5 out of the 6 remaining, R214 is deleted and only in one case, in OXA-438, the R214 is still present, but two amino acids 215-216 have been deleted (12). Changes at position R214 have a drastic impact on the hydrolysis of carbapenems because of the loss of the salt bridge with D159 (18). The β5–β6 loop extends into the outer portion of the active site crevice and defines a rather hydrophilic cavity filled with several water molecules, one of which will perform the nucleophilic attack on the acyl-enzyme intermediate in the deacylation step (15,17).

In this study, we have characterized a novel natural OXA-48 variant, OXA-933 with a D159N change. To evaluate the impact of this AA change and to further characterize the role of this position and its interaction with R214, susceptibility testing, steady state kinetic parameters together with a detailed structural analysis were performed for OXA-933 (OXA-48-D159N), and several in vitro generated OXA-48 point mutant derivatives (D159A, D159G, D159K, D159W). In addition, the genetic support of this novel OXA-48 variant was determined.

Results

K. pneumoniae 241B9 clinical isolate, antimicrobial susceptibility testing of and carbapenemase confirmation tests

The clinical *K. pneumoniae* 241B9 strain was recovered from an urinary tract infection of an hospitalized woman in a long term care facility in 2019. Disk diffusion antibiogram revealed that *K. pneumoniae* 241B9 was resistant as expected to amoxicillin, ticarcillin, and piperacillin, but also to amoxicillin/clavulanic acid, ticarcillin/clavulanic acid and piperacillin/tazobactam, likely suggesting the presence of an OXA-type acquired ß-lactamase. In addition, the isolate was also resistant to temocillin, but with a zone diameter of 13 mm, which could be compatible with an OXA-48 type variant. *K. pneumoniae* 241B9 remained susceptible to all other ß-lactams tested, including carbapenems. The zone diameter of ertapenem was slightly reduced (24 mm) and that of meropenem (28 mm) was at the EUCAST recommended screening cut-off of >0.125 µg/ml (zone diameter <28 mm). MIC testing using E-tests revealed an MIC of 0.5 µg/ml and 0.032 µg/ml for ertapenem and meropenem, respectively. The presence of a carbapenem-hydrolyzing enzyme was further searched using the Carba NP, a home-made biochemical test based on imipenem hydrolysis (19), and the immunochromatographic NG-Test Carba5 assay (NG Biotech, Guipry, France; (20). While Carba NP test was inconsistently positive, the NG-Test Carba5 was repeatedly positive for OXA-48-like enzyme.

Disc diffusion antibiogram revealed further that *K. pneumoniae* 241B9 was susceptible to all the other tested antibiotic families e.g. aminoglycosides, fluoroquinolones, chloramphenicol, tigecyclines, and colistin (confirmed by MIC testing [MIC=0.5 µg/ml]), except to rifampin.

As *K. pneumoniae* 241B9 had a reduced susceptibility toward carbapenems and temocillin, we tested its ability to grow on standard chromogenic and selective media, such as ChromID® CARBA SMART. Using an inoculum of 10^3 CFU, *K. pneumoniae* 241B9 strain

grew on both sides (Carba and OXA-48) of the ChromID® CARBA SMART plate (BioMérieux).

Genomic features of *K. pneumoniae* 241B9

WGS sequencing of *K. pneumoniae* 241B9 revealed a genome of 5,339,000-bp with a mean coverage of 90.7 X. The Multi locus sequence typing (MLST) *of K. pneumoniae* 241B9 according to MLST 1.8 software (21), revealed ST-1079 (2-5-1-1-9-1-19), an ST rarely described and with only 10 occurrences in the *Klebsiella* Pasteur MLST database over the last 15 years from Argentina, United Kingdom, France and Australia (https://bigsdb.pasteur.fr/klebsiella/).

Acquired resistance genes and point mutations involved in resistance were analyzed using ResFinder (22). The naturally occurring $bla_{\text{SHV-1}}$ gene, and a variant of $bla_{\text{OXA-48}}$ carbapenemase gene with a G_{475} to A mutation that results in D159N AA change, named $bla_{\text{OXA-933}}$ gene, were identified in this isolate. In addition, *oqxA* and *oqxB* genes were also present in the isolate, likely at the origin of reduced susceptibility to fluoroquinolones (MIC of 0.5 µg/ml to ciprofloxacin) as no chromosomal mutation was present in the QRDR region. *fosA* gene conferring resistance to fosfomycin was also present in the genome (23). In addition, point mutations were found in *ompK36* and *ompK37*, but none has been described to be involved in reduced susceptibility to third generation cephalosporins. According to PlasmidFinder (24), no plasmid replication origin could be evidenced.

Genetic support and environment of $bla_{\text{OXA-933}}$ gene

The $bla_{\text{OXA-933}}$ gene was located on Tn*2208*, a 2696-bp composite transposon made of two IS*1* elements inserted with a 9-bp target site duplication into a non-self-transmissible

plasmid resulting in plasmid pOXA-933 of 7872-bp in size. This plasmid differed only by 5 nucleotides (including the G_{475} to A mutation that resulted in D159N AA change in OXA-933) from plasmid pMTY17816 expressing OXA-48 in an MDR *K. pneumoniae* clinical isolate TUM17816 from Vietnam (AP019554) or from plasmid pIPCEC31_3 expressing OXA-48 in an *E. coli* IPCEC31 isolate from Japan (AP026786), 19 nucleotides from plasmid p53_E-OXA48 expressing OXA-48 in an *E. coli* 53 isolate from Switzerland (CP048364.1), and 24 nucleotides from plasmid pMTY17823_OXA48 isolated in *K. pneumoniae* TUM17823 from Japan (AP019557). Electroporation of this plasmid into *E. coli* TOP10 yielded transformants resistant to β-lactams and with reduced susceptibility to carbapenems (Table 1).

Phenotypical characterization of OXA-933 β-lactamase and comparison with *in vitro* generated point mutant derivatives

MICs, Carba NP test and immunochromatographic assays were performed on *E. coli* TOP10 harboring pTOPO-OXA-48, pTOPO-OXA-933 (D159N), and pTOPO-OXA-48-D159-A,-G,-K, and -W (Table 1). All the OXA-48 variants exhibited lower MICs values for penicillins and carbapenems as compared to OXA-48. In contrast, no change of MIC values for ceftazidime and cefotaxime was observed between OXA-48, OXA-933 and the four mutants. CarbaNP test revealed an inconsistent and weak positive result with the clinical strain but was negative for all the mutants except for D159G suggesting that OXA933 and OXA-48-D159G exhibited a weak imipenem hydrolysis. Finally, NG-test Carba5, an immunochromatographic assay used for detection of the most prevalent carbapenemases such as OXA-48, was positive for the clinical *K. pneumoniae* 249B1 strain, and for *E. coli* harboring pTOPO-OXA-48, pTOPO-OXA-933 (D159N), pTOPO-OXA-48-D159-A,-G, and -K, but not for pTOPO-OXA-48-D159W. Together, the lack of carbapenem-hydrolyzing activity and the absence of detection with specific

antibodies suggest that the aspartate replacement with the bulky and hydrophobic tryptophan induced a significant modification of the 3D structure of the enzyme.

MICs assays were also performed in an OmpC/OmpF porin-deficient *E. coli* HB4 strain harboring the natural pOXA-933, and pTOPO-OXA-933 (Table 1). With the natural plasmid pOXA-933, the *E. coli* HB4 was resistant to all ß-lactams tested, while *E. coli* HB4 pTOPO-OXA-933, that contains only the open reading frame of OXA-933, only reduced susceptibilities are observed, as transcription and translation are in suboptimal configuration.

Biochemical properties of OXA-933

Steady-state kinetic parameters were determined to compare the catalytic properties of OXA-933 and two in vitro generated mutants (OXA-48-D159G and OXA-48-D159K) with those of OXA-48 and OXA-244 (Table 3).

The catalytic efficiency (k_{cat}/K_m) of OXA-933 regarding ampicillin hydrolysis was 5.8-fold lower (0.413 mM-1 s-1) than that of OXA-48 (2.400 mM-1 s-1) (Table 3), comparable to OXA-244 (0.549 mM-1 s-1). In addition, hydrolysis of temocillin by OXA-933 revealed a Km and a k_{cat} 3-fold higher and 4-fold higher, respectively, thus resulting in a 2-fold higher catalytic efficiency as compared with OXA-48. This result is very different from that of OXA-244, where a 20-fold decrease was observed (9). Cefalotin is hydrolyzed with a 20-fold lower k_{cat}/K_m as compared with the value for OXA-48. Oxyimino cephalosporins, such as cefotaxime, are weakly hydrolyzed, and the k_{cat}/K_m was comparable with that of OXA-48. For ceftazidime, a bulkier oxyimino cephalosporin, no hydrolysis was observed even with 1.92 µM purified enzyme and up to 500 µM substrate (data not shown), as shown previously for OXA-48 (4,7).

Carbapenems were among the preferred OXA-48 substrates (7), with the highest catalytic efficiency (k_{cat}/K_m), observed for the hydrolysis of imipenem (0.37 10^3 mM-1s-1) (7). OXA-933 has k_{cat}/K_m values 3-fold, 20-fold and 4-fold lower for imipenem, meropenem and ertapenem hydrolysis, respectively, as compared with OXA-48. These values are similar to those observed for OXA-244, with k_{cat}/K_m values 6-fold, 14-fold, and 10-fold lower for imipenem, meropenem and ertapenem hydrolysis, respectively, as compared with OXA-48.

These reduced catalytic efficiencies for carbapenems in OXA-933 were mainly due to a reduction in the turnover number. Interestingly, as observed for OXA-232, the k_{cat}/K_m of ertapenem for OXA-933 was 480-fold lower than that of imipenem, but only slightly affected as compared with the value for OXA-48 (1 versus 0.26 mM-1 s-1). Overall, the catalytic efficiencies of OXA-48-D159G and OXA-48-D159K are similar to those of OXA-933.

Determination of IC50s showed that OXA-933 and OXA-48 were similarly inhibited by clavulanic acid (4.55 µM and 28.5 µM, respectively), tazobactam (4.23 µM and 20 µM, respectively) and avibactam (6 µM and 2 µM, respectively).

Molecular modelling. An *in-silico* study was performed to identify the structural determinants that could explain the experimentally determined differences between the hydrolytic profiles of OXA-933 and its variants in comparison with OXA-48. The three-dimensional structures of OXA-48, OXA-244 (i.e. OXA-48-R214G), OXA-933 (i.e. OXA-48-D159N), OXA-48-D159G and OXA-48-D159K were modelled, showing different conformations of key residues of the active site, and compared with the docking conformation of temocillin in the active site of OXA-48 (Figures 2 and S1). In all complexes, temocillin establishes hydrogen bonds with the backbone of Y211 and with the side chain of T209, and a

strong ionic bridge with R250. In the OXA-48 structure, R214 interacts with temocillin through a strong ionic interaction and with D159 through a hydrogen bond. A hydrogen bond is also observed between D159 and S155 (Figure 2a). The mutation R214G in OXA-244 compared with OXA-48 induces a destabilization of the interaction with temocillin, which shows a 8-fold lower affinity (Figure 2b). In OXA-933, the OD1 atom of N159 is already engaged in the hydrogen bond with S155 and no hydrogen bond is possible between the ND2 atom of N159 and the side chain of R214. Therefore, R214 would change the conformation to make simultaneously a hydrogen bond with T213 and an ionic bridge with temocillin (Figure 2c). These interactions restore almost completely the affinity of the protein for temocillin. In the absence of possible interactions between R214 and the residue in position 159, the same conformational change is also observed for the OXA-48-D159G and OXA-48-D159K mutants (Figure 2d,e), with similar effects on the affinity for temocillin. All these results are in perfect agreement with the experimental data (Table 3).

Discussion

Since the first description of an Enterobacterales producing OXA-48 (4) in 2004, a rapid dissemination has been observed, and OXA-48 producers became endemic in many countries worldwide (6). OXA-48 variants such as OXA-232, OXA-244, OXA-484 with changes at position R214 located in the β5-β6 loop display reduced hydrolytic activity especially of carbapenems and temocillin as compared to OXA-48 (7,9,13,15,16,18). This reduction in related to the absence of a salt bridge between R214 and D159 that stabilizes the shape of the active site in OXA-48 (13,15).

K pneumoniae isolate 241B9 expresses a D159N OXA-48 variant that gave an inconsistently positive Carba NP test results, suggesting imipenem-hydrolysis at the limit of

detection of the assay. These observations were in favor of the hypothesis that the D159 plays also a major role in the hydrolytic profile of OXA-48 by establishing a salt bridge with R214 to stabilize the active site for carbapenem-hydrolysis (13). To validate this hypothesis, we generated mono-mutants of OXA-48 (D159A, D159G, D159K and D159W) and analyzed MICs for ß-lactams and kinetic parameters for OXA-933, and for OXA-48-D159G and D159K. These mutations were chosen regarding their intrinsic properties: alanine and glycine as hydrophobic aliphatic small AA, tryptophan a bulky hydrophobic aromatic AA and lysine a polar positively charged AA. Thus, in comparison with OXA-48 we observed that substitution of the D159 led to an increase of susceptibility toward all the β-lactams. The D159W substitution has almost completely inactivated the β-lactamase (data not shown).

CarbaNP test revealing carbapenemase activity was evaluated on several *E. coli* TOP10 isolates expressing OXA-48, OXA-244, OXA-933 and point mutant derivatives of position D159 from pTOPO plasmids. Except for pTOPO-OXA-48 and TOP10-pTOPO-OXA-48-D159G, the Carba NP test remained repeatedly negative suggesting carbapenem-hydrolytic activity below the detection limit of the assay. All these OXA-48-variants were sufficiently expressed, as the lateral flow immunoassay NG-Test Carba5 yielded positive signals in less than 2 minutes, except for TOP10-pTOPO-OXA-48-D159W, suggesting that replacement with this bulky AA has substantially modified the structure of the protein, at least the part that is recognized by one of the antibodies included in the test.

The clinical *K. pneumoniae* 24B1strain, *E. coli* Top10 pOXA-933 and *E. coli* Top10 pTOPO-OXA-933 had different MIC values, likely due to species specific expression and impermeability problems, but all had reduced MICs as compared to OXA-48. These reductions were comparable to OXA-244 (Table 1). The MICs of the various mutants were similar to those

of OXA-933, confirming a loss of ability to hydrolyze carbapenems (Table 1). Even though temocillin MICs were much lower for OXA-933 and the generated mutants as compared to OXA-48, these results could not be confirmed through steady state kinetics determination. Similar discrepancies between MIC for temocillin and its hydrolysis have already between observed for other OXA-48-like variants (7,9,13).

Differences in catalytic efficiencies were due to changes in both K_m and k_{cat}. The steady-state kinetics of OXA-933, which differs by D159N from OXA-48, revealed that the OXA-933 active site can still accommodate carbapenem and temocillin substrates, but with decreased catalytic efficiencies as compared with OXA-48. Kinetic parameters of the OXA-48-D159G and D159K variants show overall decreased catalytic efficiencies (k_{cat}/K_m) for ampicillin, cephalotin, imipenem and meropenem, similar to OXA-933. The most significant difference was observed for meropenem, with a decrease of 15 to 20-fold. This result is a consequence of at least a 10-fold decrease of affinity. Regarding imipenem, a weak decrease of catalytic efficiency was noticed mostly due to a diminution of the turnover (k_{cat}). Thus, these results tend to show the importance of residue D159 for the hydrolysis of carbapenems. We have shown previously (9,18), that R214 could interact also with the substrate and D159. This interaction could stabilize R214 in the right position and thus stabilize the small substrates as carbapenems in the active site. S155 would also be a residue of a particular interest since it directly interacts with D159 and could be the target for further studies. Overall, OXA-933 and OXA-244, even though differing by the AA changes (R214G for OXA-244), have similar catalytic efficiency values (Table 3), further supporting the importance of the salt bridge established between these two residues. The IC50s values for clavulanic acid, tazobactam and avibactam of OXA-933, being similar to those of OXA-48, suggest that D159N is not involved in inhibition by the tested inhibitors (7,10, 25).

The structural analysis of the active sites of these mutants (Figure S1) and their interaction with temocillin (Figure 2) show important changes in the conformation and in the size of the active site induced by these mutations. In OXA-244, the active site is enlarged as a consequence of the mutation R214G and the flexibility of this region is likely to be increased in the absence of the salt bridge R214-D159. This mutation also destabilizes the interaction of temocillin, leading to a significant decrease of affinity. In OXA-933, although the mutation D159N looks minor at the first sight, it also breaks the salt bridge R214-D159, allowing the R214 to change the conformation and to interact with T213 through a hydrogen bond and with temocillin through an ionic bridge. The conformational change and interactions are also observed in the OXA-48-D159G and OXA-48-D159K mutants, leading to an important remodeling of the active site surface in this region and to the reinforcement of the interaction with temocillin. Overall, these changes in the conformation of the active site and in the interaction with temocillin are in agreement with the kinetic data determined experimentally (Table 3).

Most OXA-48-like variants are associated with different Tn*1999* variants inserted on IncL plasmids, but some such as OXA-181 and OXA-232 are associated with IS*Ecp1*, Tn*2013* on ColE2, and IncX3 types of plasmids (6,26). The pOXA-933 natural plasmid of 7872-bp in size was closely related (5-24 nucleotide differences) to plasmids carrying OXA-48 from an *K pneumoniae* clinical isolate TUM17816 from Vietnam (AP019554), an *E. coli* IPCEC31 isolate from Japan (AP026786), an *E. coli* 53 isolate from Switzerland (CP048364), and *K. pneumoniae* TUM17823 from Japan (AP019557), suggesting that this type of plasmid may have already spread on several continents and in different species. IS*1*-based composite transposons have the tendency to transpose at high frequency in Enterobacterales and could thus promote even further the spread of OXA-48 type enzymes, even beyond Enterobacterales, in a similar

manner to Tn*9* or Tn*1681*, two highly dispersed composite transposons carrying the *cat* gene, conferring chloramphenicol resistance and a heat stable toxin, respectively (27,28).

Conclusions

This study characterized a new variant of OXA-48, OXA-933 with a D159N amino acid change located outside of the ß5-ß6 loop but involved in active site stabilization through salt bridges with R214 and S155. According to Dabos *et al.* OXA-933, even though with reduced activity towards carbapenems, has still enough carbapenemase activity to be considered as a true carbapenemase, especially when expressed in bacteria with impaired outer membrane permeability (30). Nevertheless, this reduction in hydrolytic activities, especially for carbapenems and temocillin, results in detection problems using hydrolysis tests, such as Carba NP, and growth on selective medias, such as ChromID CarbaSmart biplates (bioMérieux). The use LFIA, such as NG-Test CARBA 5 may be an interesting tool to detect these OXA-48-like variants. The detection from rectal swab samples may still be possible using chromogenic selective media for *K. pneumoniae* isolates, but the situation may be different with *E. coli* isolates, as observed with OXA-244-producers (9, 31). Even though OXA-933 hydrolyses carbapenems only weakly, its transfer into a porin-deficient genetic background may yield high level of carbapenem-resistance (Table 4). Finally, OXA-933 is present on a novel composite transposon made of two IS*1* elements, Tn*2208*, inserted on a high copy number plasmid further illustrating the genetic variability associated with OXA-48 carbapenemases.

Materials and methods

Bacterial strains

Klebsiella pneumoniae 241B9 clinical isolate was identified using MALDI-TOF (MALDI Biotyper, Bruker Daltonics, Hamburg, Germany). *Escherichia coli* TOP10 (Invitrogen, Saint-Aubin, France) and *E. coli* BL21 (DE3) (Novagen, VWR International, Fontenay-sous-Bois, France) were used for cloning and over expression experiments, respectively (13).

Susceptibility testing and carbapenemase detection

Antimicrobial susceptibilities were determined by disk diffusion technique on Mueller-Hinton agar (Bio-Rad, Marnes-La-Coquette, France) and Minimal inhibitory concentration (MIC) values were determined using the Etest technique (BioMérieux, Paris, France). Susceptibility results were interpreted according to the EUCAST breakpoints, updated in 2022 (http://www.eucast.org). Detection of a carbapenemase activity were carried out with the Carba NP test as previously described (19). The Lateral flow immunoassay NG-Test® CARBA-5 (NG Biotech, Guipry, France) was used to detect members of the five main carbapenemases families (i.e., KPC-, NDM-, VIM-, IMP-, and OXA-48-like enzymes) according to the manufacturer's instructions (20).

Whole genome sequencing

Total DNA was extracted from colonies using the Ultraclean Microbial DNA Isolation Kit (MO BIO Laboratories, Carlsbad, CA, US) following the manufacturer's instructions. The DNA concentration and purity were controlled by a Qubit® 2.0 Fluorometer using the dsDNA HS and/or BR assay kit (Life technologies, Carlsbad, CA, US). The library was prepared using the NEBNext Ultra II FS DNA Library Prep Kit for Illumina (NEB, France) according to the manufacturer's instructions. Whole genome sequencing was performed on an Illumina NextSeq 500 instrument (Illumina). De novo assembly was performed by CLC genomics 10.2 program (Qiagen, Les Ulis, France), and the genomes were analyzed online using software available at

339 the Center for Genomic Epidemiology-CGE (https://cge.food.dtu.dk/services/ResFinder/). The
340 acquired antimicrobial resistance genes were identified by uploading the assembled genomes to
341 the Resfinder server v2.1 (http://cge.cbs.dtu.dk/services/ResFinder-2.1) (22). The Multi Locus
342 Sequence Typing (MLST) and the identification of the different plasmids were also obtained by
343 uploading the assembled genomes to the MLST 1.8 (21) and PlasmidFinder 1.3 (24) servers,
344 respectively, available at https://cge.cbs.dtu.dk/services/.

345 **Plasmid characterization**

346 Plasmid DNA of the clinical isolate *K. pneumoniae* 241B9 was extracted using the Kieser
347 method (32) and electroporated into *E. coli* TOP10 strain by electroporation (GenePulser,
348 Biorad, Marne-La-Coquette, France) as previously described (13). Plasmids of parental *K.*
349 *pneumoniae* 241B9 isolate and transformants were analyzed on 0.7% agarose gel stained with
350 ethidium bromide. Plasmids of ca. 154, 66, 48, and 7 kb of *E. coli* NCTC 50192 were used as
351 plasmid size markers (13).

352 **Site directed mutagenesis**

353 Site-directed mutagenesis was done using the QuikChange II site-directed mutagenesis kit
354 (Agilent Technologies, Les Ulis, France) as recommended the manufacturer's protocol, and the
355 pTOPO-$bla_{\text{OXA-48}}$ plasmid as a template (18). Specific primers used for the different mutations,
356 were designed using the QuikChange Primer Design software (Agilent Technologies) (Table
357 S1): Plasmids pTOPO-OXA-48-D159G, pTOPO-OXA-48-D159A, pTOPO-OXA-48-D159K
358 and pTOPO-OXA-48-D159W were then electroporated into *E. coli* TOP10 and the presence of
359 the mutation was confirmed by Sanger sequencing using an ABI Prism 3100 sequencer (Applied
360 Biosystems, Les Ulis, France) as previously described (7).

361 **PCR and cloning experiments**

Total DNAs of *K. pneumoniae* 241B9 isolate extracted using the QIAamp DNA mini kit (Qiagen, Courtaboeuf, France) was used as templates for PCR amplication of $bla_{\text{OXA-933}}$ gene using the Phusion High-Fidelity DNA Polymerase (ThermoFischer Scientific, Villebon-sur-Yvette, France) and OXA-48A and OXA-48B primers (Table S1). The amplicon obtained was then cloned into the pCR®-Blunt II-TOPO® plasmid (Invitrogen, Illkirch, France), downstream of the pLac promoter, in the same orientation, resulting in pOXA-933 as previously described (18). The $bla_{\text{OXA-933}}$, $bla_{\text{OXA-48-D159G}}$, and $bla_{\text{OXA-48-D159K}}$ gene fragments were amplified using primers INF-48 F and INF-48 R (Table S1) corresponding to the mature β-lactamase and cloned into the expression vector pET41b (+) (Novagen, VWR International, Fontenay-sous-Bois, France) as previously described (18). The recombinant plasmid pET41-OXA-933, pET41-OXA-48-D159G, and pET41-OXA-48-D159K were then transformed into the chemically competent *E. coli* strain BL21 (DE3) (Novagen).

Recombinant plasmids were verified by Sanger on an automated ABI Prism 3100 sequencer (Applied Biosystems, Les Ulis, France) as previously described (18). Nucleotide sequences were analyzed using software available at the National Center for Biotechnology Information website (https://www.ncbi.nlm.nih.gov).

β-Lactamase production and purification

Overnight cultures of *E. coli* BL21(DE3) harboring recombinant plasmid pET41b-OXA-933, pET41b-OXA-48-D159G and pET41b-OXA-48-D159K were used to inoculate 2 liters of LB medium broth containing 50 µg/ml of kanamycin. Bacteria were grown at 37 °C until OD_{600} of 0.6 is reached and expression of the OXA-48 mutants was induced overnight at 25 °C with 0.2 mM IPTG. Purification of OXA-933, OXA-48-D159G and OXA-48-D159K was done as previously described (7,13). Protein purity was estimated by SDS-PAGE, pure fractions were

pooled and dialyzed against 100 mM sodium phosphate, 50 mM K_2SO_4 (pH 7.0) and concentrated using Vivaspin® 10 kDa columns (GE Healthcare, Freiburg, Germany). Protein concentration was determined by Bradford Protein assay (Bio-Rad) (13).

Steady-state kinetic parameters

The k_{cat} and K_m values of purified OXA-933, OXA-48-D159K and OXA-48-D159G were determined at 30°C in 100 mM sodium phosphate buffer (pH 7.0) as previously described (7,13). The β-lactams were purchased from Sigma–Aldrich (Saint-Quentin-Fallavier, France). Comparative activation of OXA-933 by CO_2 was conducted by monitoring the rate of hydrolysis of penicillins in the same buffer supplemented with 50 mM sodium hydrogen carbonate ($NaHCO_3$) as the source of CO_2 (7,9). OXA-48 and OXA-244 kinetic parameters, used in the comparison, were previously determined by Docquier et al. and Rima et al., respectively (9,15).

Molecular modelling

UCSF Chimera package (33) was used for structural analysis and image plotting. The three-dimensional structures were generated by homology modeling using MODELLER version 10.3 (34) and the structure 6PQI (35) as template, or directly from sequence using AlphaFold (36), through a local implementation of ColabFold (37). Three-dimensional structures of the β-lactam ligands were generated using the Corina (version 3.60) program (Molecular Networks GmbH, Erlangen, Germany). Molecular docking calculations were performed using the Gold program (Cambridge Crystallographic Data Centre, Cambridge, UK) (38) and the GoldScore scoring function. The binding site, defined as a 20-Å-radius sphere, was centred on the OG oxygen atom of Ser70. All other parameters had default values.

Nucleotide sequence accession numbers

The nucleotide sequence of the *bla*$_{\text{OXA-933}}$ gene and pOXA-933 have been submitted to the EMBL/Genbank nucleotide sequence database under the accession number MW073108 and OQ915017, respectively. The Whole Genome Sequencing data of *K. pneumoniae* 241B9 has been deposited at the DDBJ/ENA/GenBank under the accession code JARYTJ000000000.

Acknowledgments

This work was supported by the Assistance Publique – Hôpitaux de Paris (AP-HP), the University Paris-Saclay, INSERM, and by grants from the French National Research Agency [ANR-19-AMRB-0004 and ANR-20-PAMR-0010). LD, TN and BII are members of ESCMID Study Group for Antimicrobial Resistance Surveillance - ESGARS.

Conflicts of interest

None to disclose.

References

1. Bonomo RA, Burd EM, Conly J, Limbago BM, Poirel L, Segre JA, Westblade LF. 2018. Carbapenemase-Producing Organisms: A Global Scourge. Clin Infect Dis 66:1290-1297.
2. Hammoudi Halat D, Ayoub Moubareck C. 2020. The Current Burden of Carbapenemases: Review of Significant Properties and Dissemination among Gram-Negative Bacteria. Antibiotics (Basel, Switzerland). 9:186
3. Queenan AM, Bush K. Carbapenemases: the versatile beta-lactamases. 2007. Clin Microbiol Rev. 20: 440-58.
4. Poirel L, Héritier C, Tolün V, Nordmann P. 2004. Emergence of oxacillinase-mediated resistance to imipenem in Klebsiella pneumoniae. Antimicrob Agents Chemother 48: 15-22.

5. Aubert D, Naas T, Héritier C, Poirel L, Nordmann P. 2006. Functional characterization of IS1999, an IS4 family element involved in mobilization and expression of beta-lactam resistance genes. J Bacteriol 188: 6506-14.

6. Pitout JDD, Peirano G, Kock MM, Strydom KA, Matsumura Y. 2019. The Global Ascendency of OXA-48-Type Carbapenemases. Clin Microbiol Rev 33:e00102-19.

7. Oueslati S, Nordmann P, Poirel L. 2015. Heterogeneous hydrolytic features for OXA-48-like β-lactamases. J Antimicrob Chemother 70: 1059-63.

8. Naas T, Oueslati S, Bonnin RA, Dabos ML., Zavala A, Dortet L, Retailleau P, Iorga BI. 2017. Beta-Lactamase DataBase (BLDB) - Structure and Function. J Enz Inh Med Chem 32:917-919.

9. Rima M, Emeraud C, Bonnin RA, Gonzalez C, Dortet L, Iorga BI, Oueslati S, Naas T. 2021. Biochemical characterization of OXA-244, an emerging OXA-48 variant with reduced β-lactam hydrolytic activity. J Antimicrob Chemother 76:2024-2028.

10. Oueslati S, Retailleau P, Marchini L, Dortet L, Bonnin RA, Iorga BI, Naas T. 2019. Biochemical and Structural Characterization of OXA-405, an OXA-48 Variant with Extended-Spectrum β-Lactamase Activity. Microorganisms 8:24.

11. Poirel L, Castanheira M, Carrër A, Rodriguez CP, Jones RN, Smayevsky J, Nordmann P. 2011. OXA-163, an OXA-48-related class D β-lactamase with extended activity toward expanded-spectrum cephalosporins. Antimicrob Agents Chemother 55: 2546-51.

12. De Belder D, Ghiglione B, Pasteran F, de Mendieta JM, Corso A, Curto L, Di Bella A, Gutkind G, Gomez SA, Power P. 2020. Comparative Kinetic Analysis of OXA-438 with Related OXA-48-Type Carbapenem-Hydrolyzing Class D β-Lactamases. ACS Infect Dis 6:3026-33.

13. Dabos L, Raczynska JE, Bogaerts P, Zavala A, Girlich D, Bonnin RA, Dortet L, Peyrat A, Retailleau P, Iorga BI, Jaskólski M, Glupczynski Y, Naas T. 2023. Structural and Biochemical Features of OXA-517: a Carbapenem and Expanded-Spectrum Cephalosporin Hydrolyzing OXA-48 Variant. Antimicrob Agents Chemother 67:e0109522.
14. Dabos L, Bonnin RA, Dortet L, Naas T. 2021. OXA-793, a carbapenem, expanded-spectrum cephalosporin and aztreonam hydrolysing OXA-48 variant. 2023. O2981 ePoster, ECCMID Online.
15. Docquier JD, Calderone V, De Luca F, Benvenuti M, Giuliani F, Bellucci L, Tafi A, Nordmann P, Botta M, Rossolini GM, Mangani S. 2009. Crystal structure of the OXA-48 beta-lactamase reveals mechanistic diversity among class D carbapenemases. Chem Biol 16:540-7.
16. Dabos L, Zavala A, Bonnin RA, Beckstein O, Retailleau P, Iorga BI, Naas T. 2020. Substrate Specificity of OXA-48 after β5-β6 Loop Replacement. ACS Infect Dis 6:1032-43.
17. Smith CA, Stewart NK, Toth M, Vakulenko SB. 2019. Structural Insights into the Mechanism of Carbapenemase Activity of the OXA-48 β-Lactamase. Antimicrob Agents Chemother 63:e01202-19.
18. Oueslati S, Retailleau P, Marchini L, Berthault C, Dortet L, Bonnin RA, Iorga BI, Naas T. 2020. Role of Arginine 214 in the Substrate Specificity of OXA-48. Antimicrob Agents Chemother 64:e02329-19.
19. Dortet L, Agathine A, Naas T, Cuzon G, Poirel L, Nordmann P. 2015. Evaluation of the RAPIDEC® CARBA NP, the Rapid CARB Screen® and the Carba NP test for

biochemical detection of carbapenemase-producing Enterobacteriaceae. J Antimicrob Chemother 70:3014-22.

20. Boutal H, Vogel A, Bernabeu S, Devilliers K, Creton E, Cotellon G, Plaisance M, Oueslati S, Dortet L, Jousset A, Simon S, Naas T, Volland H. 2018. A multiplex lateral flow immunoassay for the rapid identification of NDM-, KPC-, IMP- and VIM-type and OXA-48-like carbapenemase-producing Enterobacteriaceae. J Antimicrob Chemother 73: 909-15.

21. Larsen MV, Cosentino S, Rasmussen S, Friis C, Hasman H, Marvig RL, Jelsbak L, Sicheritz-Pontén T, Ussery DW, Aarestrup FM, Lund O. 2012. Multilocus sequence typing of total-genome-sequenced bacteria. J Clin Microbiol 50: 1355-61.

22. Bortolaia V KR, Ruppe E, Roberts MC, Schwarz S, Cattoir V, Philippon A, Allesoe RL, Rebelo AR, Florensa AR, Fagelhauer L, Chakraborty T, Neumann B, Werner G, Bender JK, Stingl K, Nguyen M, Coppens J, Xavier BB, Malhotra-Kumar S, Westh H, Pinholt M, Anjum MF, Duggett NA, Kempf I, NykÃ¤senoja S, Olkkola S, Wieczorek K, Amaro A, Clemente L, Mossong J, Losch S, Ragimbeau C, Lund O, Aarestrup FM. 2020. Resfinder 4.0 for predictions of phenotypes from genotypes. J Antimicrob Chemother 75: 3491-500.

23. Ito R, Mustapha MM, Tomich AD, Callaghan JD, McElheny CL, Mettus RT, Shanks RMQ, Sluis-Cremer N, Doi Y. 2017. Widespread Fosfomycin Resistance in Gram-Negative Bacteria Attributable to the Chromosomal fosA Gene. mBio 8:e00749-17.

24. Carattoli A, Zankari E, García-Fernández A, Voldby Larsen M, Lund O, Villa L, Møller Aarestrup F, Hasman H. 2014. In silico detection and typing of plasmids using PlasmidFinder and plasmid multilocus sequence typing. Antimicrob Agents Chemother 58:3895-903.

498 25. Fröhlich C, Sørum V, Thomassen AM, Johnsen PJ, Leiros HKS, Samuelsen O. 2019.
499 OXA-48-Mediated Ceftazidime-Avibactam Resistance Is Associated with Evolutionary
500 Trade-Offs. Msphere; 4: e00024-19.
501 26. Poirel L, Bonnin RA, Nordmann P. 2012. Genetic features of the widespread plasmid
502 coding for the carbapenemase OXA-48. Antimicrob Agents Chemother 56: 559-62.
503 27. Matthews PR, Cameron FH, Stewart PR. 1983. Occurrence of chloramphenicol
504 acetyltransferase and Tn9 among chloramphenicol-resistant enteric bacteria from humans
505 and animals. J Antimicrob Chemother 11:535-42.
506 28. Zsolt Fekete P, Schneider G, Olasz F, Blum-Oehler G, Hacker JH, Nagy B. 2003.
507 Detection of a plasmid-encoded pathogenicity island in F18+ enterotoxigenic and
508 verotoxigenic Escherichia coli from weaned pigs. Int J Med Microbiol 293:287-98.
509 29. Dabos L, Bogaerts P, Bonnin RA, Zavala A, Sacré P, Iorga BI, Huang DT, Glupczynski Y,
510 Naas T. 2018. Genetic and Biochemical Characterization of OXA-519, a Novel OXA-48-
511 Like β-Lactamase. Antimicrob Agents Chemother 62:e00469-18.
512 30. Dabos L, Oueslati S, Bernabeu S, Bonnin RA, Dortet L, Naas T. 2022. To Be or Not to Be
513 an OXA-48 Carbapenemase. Microorganisms 10:25829.
514 31. Emeraud C, Biez L, Girlich D, Jousset AB, Naas T, Bonnin RA, Dortet L. 2020. Screening
515 of OXA-244 producers, a difficult-to-detect and emerging OXA-48 variant? J Antimicrob
516 Chemother 75: 2120-2123.29.
517 32. Kieser T. 1984. Factors affecting the isolation of CCC DNA from Streptomyces lividans
518 and Escherichia coli. Plasmid 12:19–36.

519 33. Pettersen EF, Goddard TD, Huang CC, Couch GS, Greenblatt DM, Meng EC, Ferrin TE.
520 2004. UCSF Chimera--a visualization system for exploratory research and analysis. J
521 Comp Chem 25: 1605-12.
522 34. Verdonk ML, Cole JC, Hartshorn MJ, Murray CW, Taylor RD. 2003. Improved protein-
523 ligand docking using GOLD. Proteins. 52: 609-23.
524 35. Sali A, Blundell TL. 1993. Comparative protein modelling by satisfaction of spatial
525 restraints. J Mol Biol 234: 779-815.
526 36. Jumper J, Evans R, Pritzel A, Green T, Figurnov M, Ronneberger O, Tunyasuvunakool K,
527 Bates R, Žídek A, Potapenko A, Bridgland A, Meyer C, Kohl SAA, Ballard AJ, Cowie A,
528 Romera-Paredes B, Nikolov S, Jain R, Adler J, Back T, Petersen S, Reiman D, Clancy E,
529 Zielinski M, Steinegger M, Pacholska M, Berghammer T, Bodenstein S, Silver D, Vinyals
530 O, Senior AW, Kavukcuoglu K, Kohli P, Hassabis D. 2021. Highly accurate protein
531 structure prediction with AlphaFold. Nature. 596: 583-9.
532 37. Mirdita M, Schütze K, Moriwaki Y, Heo L, Ovchinnikov S, Steinegger M. 2022.
533 ColabFold: making protein folding accessible to all. Nat Meth 19: 679-82.
534 38. Verdonk ML, Cole JC, Hartshorn MJ, Murray CW, Taylor RD. 2003. Improved protein–
535 ligand docking using GOLD. Proteins Struct Funct Bioinform 52:609–623.
536

Table 1: CarbaNP assay, NG test Carba5 results and MICs of β-lactams for *K. pneumoniae* 241B9 clinical strain, *E. coli* HB4 with the natural plasmid pOXA-933, with pTOPO-OXA-933, *E. coli* HB4 alone and *E. coli* TOP10 expressing OXA-48, OXA-933, OXA-48-D159K, OXA-48-D159G, OXA-48-D159W and OXA-48-D159A. [a]; OXA-244; [b]; OXA-933.

	MIC (µg/mL)											
	K. pneumoniae 241B9	*E. coli* HB4			*E. coli* TOP10							
	OXA-933 SHV-1	pOXA-933	pTOPO-OXA-933	-	pTOPO-OXA-48	pTOPO-OXA-48-R214G[a]	pTOPO-OXA48-D159N[b]	pTOPO-OXA-48-D159K	pTOPO-OXA-48-D159G	pTOPO-OXA-48 D159W	pTOPO-OXA-48 D159A	
Amoxicillin	>256	>256	>256	24	>256	>256	12	12	24	4	12	2
Piperacillin	128	>256	6	4		>256						
Ticarcillin/clavulanic acid	>256	>256	>256	12								
Temocillin	128				>256	16	12	12	12	12	4	4
Ceftazidime	<0.25	2	0.5	0.5	0.19	0.19	0.125	0.19	0.19	0.19	0.19	0.12
Cefotaxime	<0.25				0.06	0.047	0.06	0.06	0.06	0.06	0.06	0.06
Cefepime	0.094	8	0.5	0.5		0.064						
Imipenem	0.25	>32	0.16	0.125	0.75	0.25	0.25	0.25	0.25	0.25	0.25	0.25
Meropenem	0.016	32	0.25	0.25	0.25	0.016	0.032	0.016	0.023	0.016	0.016	0.016
Ertapenem	0.5	>256	32	1	0.25	0.064	0.003	0.003	0.003	0.003	0.003	0.003
CarbaNP test	+/-	-	-	-	+	+/-	-	-	+	-	-	-
NG-Test CARBA 5	OXA	OXA	OXA	-	OXA	OXA	OXA	OXA	OXA	-	OXA	-

Table 2: Steady-state kinetic parameters for hydrolysis of ß-lactam substrates by OXA-933, OXA-D159G, OXA-D159K, OXA-244 and OXA-48.

	K_m (µM)					k_{cat} (s^{-1})					k_{cat}/K_m ($mM^{-1}.s^{-1}$)				
Enzyme	OXA-48[a]	OXA-48 R214G[b]	OXA-48 D159N[c]	OXA-48 D159G	OXA-48 D159K	OXA-48	OXA-48 R214G[a]	OXA-48 D159N[b]	OXA-48 D159G	OXA-48 D159K	OXA-48	OXA-48 R214G[a]	OXA-48 D159N[b]	OXA-48 D159G	OXA-48 D159K
Benzylpenicillin	NA	450 ± 40	88 ± 9	64 ± 48	48 ± 5	NA	72 ± 8	126 ± 6	6.2 ± 4	69 ± 17	NA	163 ± 30	1450 ± 199	133 ± 14	1445 ± 256
Ampicillin	400	657 ± 160	392 ± 103	ND	ND	955	373 ± 158	152 ± 32	ND	ND	2400	549 ± 130	413 ± 147	ND	ND
Temocillin	45	364 ± 20	125 ± 9	86 ±90	35 ± 6	0.3	0.11 ± 0.02	1.4 ± 0.03	0.74 ± 0.9	0.6 ± 0.03	6	0.31 ± 0.05	11 ± 0.8	7 ± 2	19 ± 3.6
Cephalothin	195	88 ± 30	788 ± 33	85 ± 19	152 ± 75	44	3.3 ± 0.8	7.4 ± 1.6	2.4 ± 0.4	3.8 ± 1.3	225	39 ± 4	10 ± 2.4	29 ± 7	29 ± 18
Cefotaxime	>900	>1000	321 ± 72	248 ± 155	104 ± 24	>900	ND	11 ± 8	1.2 ± 0.34	0.9 ± 0.2	10	ND	32 ± 21	6 ± 3	9 ± 1.4
Imipenem	13	0.5 ± 0.2	22 ± 7	48 ± 9	5 ± 0.4	5	0.02 ± 0.001	1.8 ± 1.6	2.5 ± 0.4	0.6 ± 0.12	370	38 ± 10	125 ± 35	52 ± 1.5	120 ± 16
Meropenem	10	23 ± 4	160 ± 46	193 ±104	103 ± 10	0.07	0.02 ± 0.001	0.05 ± 0.002	0.08 ± 0.03	0.04 ± 0.002	6	0.8 ± 0.2	0.3 ± 0.09	0.4 ± 0.1	0.4 ± 0.02
Ertapenem	100	22.9 ± 0.3	200 ± 67	154 ± 110	150 ± 28	0.13	0.02 ± 0.01	0.05 ± 0.007	0.074 ± 0.02	0.11 ± 0.06	1	0.1 ± 0.03	0.26 ± 0.06	0.6 ± 0.2	0.75 ± 0.4

[a] OXA-48 values were retrieved from Docquier *et al*. (15); [b] data for OXA-244 were from Rima *et al.* (9); [c] correspond to OXA-933; [d]: NA, not available; [e]: ND, not determined. Data are the mean of three independent experiments.

Legends to figures

Figure 1: Map of the natural plasmid pOXA-933 carrying *bla*$_{\text{OXA-933}}$ gene located on Tn*2208.*

Figure 2: Docking conformation of temocillin (non-covalent binding) on OXA-48 (**a**), OXA-244 (**b**), OXA-933 (**c**), OXA-48-D159G (**d**) and OXA-48-D159K (**e**). The residue Ser70 is colored in green. The black strings represent hydrogen bonds.

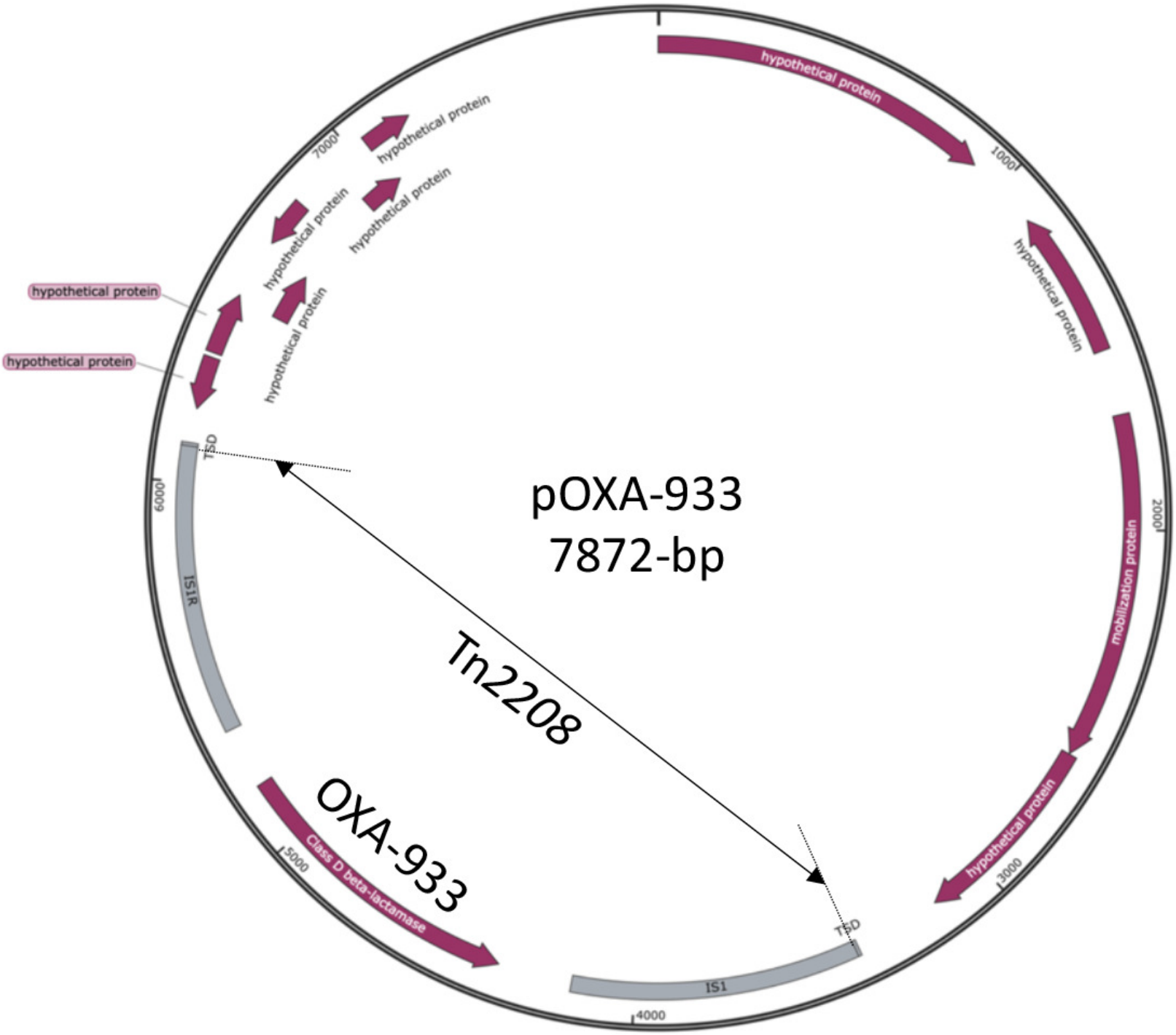
pOXA-933
7872-bp
Tn2208
OXA-933
hypothetical protein
hypothetical protein
hypothetical protein
hypothetical protein
hypothetical protein
hypothetical protein
hypothetical protein
hypothetical protein
hypothetical protein
mobilization protein
hypothetical protein
Class D beta-lactamase
IS1R
IS1
Tn2
Tn2
1000
2000
3000
4000
5000
6000
7000

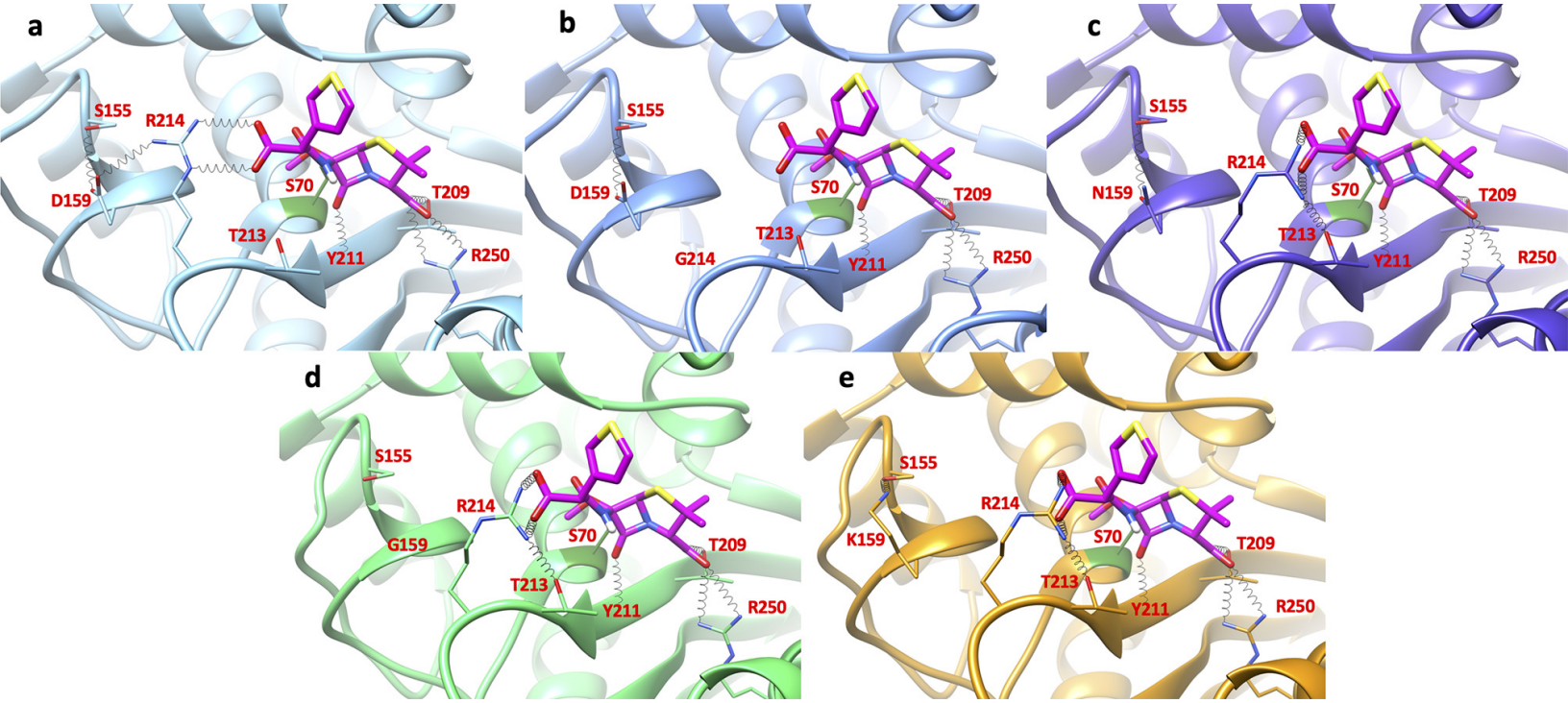
a
S155
R214
D159
S70
T209
T213
Y211
R250
b
S155
D159
S70
T209
T213
G214
Y211
R250
c
S155
R214
N159
S70
T209
T213
Y211
R250
d
S155
R214
G159
S70
T209
T213
Y211
R250
e
S155
R214
K159
S70
T209
T213
Y211
R250

Table S1 : Primers used in this study
for site directed mutagenesis

D159Aa	5'- CGAAATTCGAATACCACCGGCGAGCCAGAAACTGTCTACA-3'
D159Ab	5'- TGTAGACAGTTTCTGGCTCGCCGGTGGTATTCGAATTTCG-3'
D159Ka	5'- GAAATTCGAATACCACCCTTGAGCCAGAAACTGTCTA-3'
D159Kb	5'- TAGACAGTTTCTGGCTCAAGGGTGGTATTCGAATTTC-3'
D159Wa	5'- GGCCGAAATTCGAATACCACCCCAGAGCCAGAAACTGTCTACATT-3'
D159Wb	5'- AATGTAGACAGTTTCTGGCTCTGGGGTGGTATTCGAATTTCGGCC-3'
D159Ga	5'- CGAAATTCGAATACCACCGCCGAGCCAGAAACTGTCTACA-3'
D159Gb	5'- TGTAGACAGTTTCTGGCTCGGCGGTGGTATTCGAATTTCG-3'

For OXA-48 cloning into pTOPO

OXA-48A	5′-TTGGTGGCATCGATTATCGG-3′
OXA-48B	5′-GAGCACTTCTTTTGTGATGGC-3′

For OXA-48-cloning in pET41b

INF-48 F	5'-AAGGAGATATACATATGGTAGCAAAGGAATGGCAAG-3'
INF-48 R	5'-GGTGGTGGTGCTCGAAGGGAATAATTTTTTCCTGTTTGAG-3'

Legend to Figure S1: Docking conformation of temocillin (non-covalent binding) on OXA-48 (**a**), OXA-244 (**b**), OXA-933 (**c**), OXA-48-D159G (**d**) and OXA-48-D159K (**e**), in surface representation. The surface of residues in positions 155, 159, 213 and 214 is partially transparent to show the conformation of the corresponding residues, represented as sticks. The surface of Ser70 is colored in green. The black strings represent hydrogen bonds.